Residual trapping, solubility trapping and capillary pinning complement each other to limit CO[subscript 2] migration in deep saline aquifers

Available online at www.sciencedirect.com

ScienceDirect

Energy Procedia 63 (2014) 3833 – 3839

Energy Procedia

GHGT-14

Residual trapping, solubility trapping and capillary pinning complement each other to limit CO_2 migration in deep saline aquifers

Benzhong Zhao[a], Christopher W. MacMinn[b], Ruben Juanes[a]*

[a]*Massachusetts Institute of Technology, 77 Massachusetts Ave, Bldg. 48-319, Cambridge, MA 02139, USA*
[b]*University of Oxford, Parks Road, Oxford OX1 3PJ, UK.*

Abstract

We derive a theoretical model for the post-injection migration of a CO_2 gravity current in a confined, sloping aquifer under the influence of residual trapping, solubility trapping, and capillary pinning. The resulting model consists of two coupled partial differential equations that describe the local thickness of the buoyant CO_2 current and the thickness of the mound of brine saturated with dissolved CO_2 as a function of time. We apply this model to a representative geological formation and provide estimates of the lifetime of the buoyant CO_2 current and its maximum migration distance. Our analysis shows that residual trapping, solubility trapping, and capillary pinning complement each other in limiting the ultimate migration distance of CO_2 gravity currents. The relative contribution of residual trapping, solubility trapping, and capillary pinning varies as a function of the injection volume. Our model can be used as a screening tool to evaluate the potential of deep saline aquifers for large-scale CO_2 sequestration.

Peer-review under responsibility of the Organizing Committee of GHGT-12

Keywords: Geologic storage; capillary trapping; capillary pinning; convective dissolution; post-injection; sharp-interface; migration distance

* Corresponding author. Tel.: +1-617-253-7191; fax: +1-617-258-8850.
E-mail address: juanes@mit.edu

Peer-review under responsibility of the Organizing Committee of GHGT-12
doi:10.1016/j.egypro.2014.11.412

1. Introduction

Gravity currents in porous media have attracted much interest in the context of geological carbon dioxide (CO_2) storage, where supercritical CO_2 is captured from the flue gas of power plants and injected underground into deep saline aquifers [1-4]. Saline aquifers are geologic layers of permeable rock located 1 to 3 km below the surface, saturated with salty groundwater, and, in general, lined on top by a layer of much less permeable "caprock" [5]. They have been considered as ideal storage sites for CO_2 (see, e.g., [3,4]) due to their geologic prevalence around the globe, as well as their large storage capacity [6,7]. At reservoir conditions, CO_2 is less dense than the ambient groundwater. As a result, it will migrate upward due to buoyancy and spread along the caprock. Capillarity can be important in the spreading and migration of the buoyant CO_2 after injection, because the typical pore size is very small (~10 - 100 μm), but the impact of capillarity on these flows is not well understood.

In previous studies [8,9], we studied the impact of capillarity on the buoyant spreading of a finite-size current of non-wetting fluid into a dense, wetting fluid in a vertically confined aquifer. We demonstrated via simple table-top experiments in packings of glass beads that capillary pressure hysteresis pins a portion of the fluid-fluid interface. We showed that capillary pressure hysteresis in this system is caused by the fundamental difference in the pore-scale invasion patterns between drainage and imbibition, and is present even in the absence of contact angle hysteresis. The length of the pinned interface scales with the relative importance of capillary and gravity forces. The horizontal extent of the pinned portion of the interface grows with time and this is responsible for ultimately limiting the spreading of the buoyant current to a finite distance. This is in stark contrast to miscible gravity currents, which in the absence of diffusion, spreads forever. We developed a theoretical model that captures the evolution of immiscible gravity currents and predicts the maximum migration distance.

Other physical mechanisms such as residual trapping, where tiny blobs of CO_2 are immobilized by capillary forces, and solubility trapping, where CO_2 dissolves into the ambient groundwater, also play important roles in the migration of CO_2 gravity currents. The goal of this paper is to derive a theoretical model for the post-injection migration of a CO_2 gravity current in a confined, sloping aquifer under the combined influence of residual trapping, solubility trapping, and capillary pinning.

2. Mathematical Model

The study of gravity currents under the general framework of sharp interface models has received renewed attention in the context of geologic CO_2 sequestration in the past decade. Sharp interface models are able to simulate flow over large distances due to their relatively low computational cost compared to full numerical simulations, and they can be formulated to include the trapping mechanisms encountered in CO_2 storage. In particular, residual trapping is accounted for by incorporating a discontinuous coefficient on the accumulation term of the sharp interface model [10-12]. Solubility trapping can be modeled by incorporating convective dissolution as a constant flux of CO_2 per unit length of CO_2–brine interface [13-17]. The rate of convective dissolution slows down as the brine underneath the CO_2 current becomes saturated with dissolved CO_2, a process known as convective shutdown [18-20]. *Hidalgo et al.* (2013) [17] demonstrated that this decrease in dissolution rate can be effectively captured by modeling the CO_2 current and the CO_2-rich brine layer as a coupled system, and assuming that convective dissolution shuts down once the layer of brine saturated with CO_2 fills the region beneath the buoyant CO_2. *Zhao et al.* (2014) [9] developed a model that captures capillary pinning of immiscible gravity currents and predicts the maximum migration distance.

Here, we present a theoretical model that incorporates residual trapping, solubility trapping and capillary pinning. The complete derivation of the model and the details of the underlying assumptions will be given in a future publication. The model consists of two coupled partial differential equations that describe the evolution of the buoyant CO_2 current and the mound of brine saturated with dissolved CO_2 (hereafter referred to as the dense mound)

$$\frac{\partial h_g}{\partial t}+\frac{\kappa\lambda_g\Delta\rho_{gw}g}{(1-S_{wc}-S_{gr}\tilde{R})\phi}\frac{\partial}{\partial x}\left[(1-f_g)h_g(\sin\theta-\cos\theta\frac{\partial h_g}{\partial x}-\frac{1}{\Delta\rho_{gw}g\cos\theta}\frac{\partial P_c}{\partial x})\right]$$
$$+\frac{\kappa\lambda_d\Delta\rho_{wd}g}{(1-S_{wc}-S_{gr}\tilde{R})\phi}\frac{\partial}{\partial x}\left[f_g h_d(\sin\theta+\cos\theta\frac{\partial h_d}{\partial x})\right]=-\frac{q_d}{\phi}\varepsilon, \tag{1}$$

and

$$\frac{\partial h_d}{\partial t}-\frac{\kappa\lambda_g\Delta\rho_{gw}g}{\phi}\frac{\partial}{\partial x}\left[f_d h_g(\sin\theta-\cos\theta\frac{\partial h_g}{\partial x}-\frac{1}{\Delta\rho_{gw}g\cos\theta}\frac{\partial P_c}{\partial x})\right]$$
$$-\frac{\kappa\lambda_d\Delta\rho_{wd}g}{\phi}\frac{\partial}{\partial x}\left[(1-f_d)h_d(\sin\theta+\cos\theta\frac{\partial h_d}{\partial x})\right]=\frac{q_d(1-S_{wc}-S_{gr}\tilde{R})}{\phi\chi_v}\varepsilon, \tag{2}$$

where h_g and h_d are the local thickness of the CO_2 current and the thickness of the dense mound. κ is the intrinsic permeability of the aquifer, ϕ is the porosity of the aquifer, and θ is the slope of the aquifer. $\lambda_g = k_{rg}/\mu_g$ and $\lambda_d = k_{rd}/\mu_d$ are the mobilities of the CO_2 current and dense mound respectively. μ_g, μ_d and k_{rg}, k_{rd} are the dynamic viscosities and the relative permeabilities of the respective fluid phases. $\Delta\rho_{gw}$ is the density difference between the buoyant CO_2 and the ambient brine, $\Delta\rho_{wd}$ is the density difference between the ambient brine and the dense mound. S_{wc} is the connate water saturation, which represents the fraction of pore space occupied by immobile brine. Similarly, S_{gr} is the residual gas saturation, which represents the fraction of pore space occupied by trapped blobs of CO_2. The discontinuous coefficient $\tilde{R}$ captures the fact that residual trapping only occurs in areas where the bulk CO_2 current has been displaced by brine through imbibition. Hence, $\tilde{R}=1$ if $\partial h_g/\partial t<0$, and $\tilde{R}=0$ if $\partial h_g/\partial t\geq 0$. The local capillary pressure across the CO_2/brine interface P_c is given by the Young-Laplace equation and $P_c\sim\gamma/d$, where γ is the interfacial tension between CO_2 and brine, d is the mean grain size of the porous media. We take P_c to be constant and equal to a characteristic imbibition capillary pressure where the CO_2 current is displaced by brine. Similarly, we take P_c to be constant and equal to the drainage capillary pressure where the CO_2 current displaces the ambient brine [8,9]. Along the pinned interface, P_c transitions from the imbibition capillary pressure to the drainage capillary pressure. This transition in capillary pressure is offset by the change in hydrostatic pressure along the pinned interface, with a corresponding difference in interface height of $\Delta h_c=\Delta P_c/\Delta\rho_{gw}g\cos\theta$. Hence, the length of the pinned interface $\Delta h_c\sim \mathrm{Bo}^{-1}=\gamma/\Delta\rho_{gw}gHd$, where H is the thickness of the aquifer. The fractional flow functions f_g and f_d are given by

$$f_g=\frac{h_g\lambda_g}{h_g\lambda_g+h_d\lambda_d+\lambda_w(H-h_g-h_d)},\qquad f_d=\frac{h_d\lambda_d}{h_g\lambda_g+h_d\lambda_d+\lambda_w(H-h_g-h_d)}. \tag{3}$$

q_d is the volumetric rate of convective dissolution per unit area of fluid-fluid interface, and is given by

$$q_d=\alpha\chi_v\Delta\rho_{wd}g\kappa\lambda_d, \tag{4}$$

where α is a constant roughly equal to 0.01 [21] and χ_v is the solubility of CO_2 in brine, expressed as the volume of free-phase CO_2 that can be dissolved per unit volume of brine saturated with CO_2 [7,14]. The discontinuous coefficient ε captures the fact that convective dissolution shuts down locally where the CO_2 saturated dense mound

fills the aquifer beneath the buoyant CO_2 current [15,17]. Hence, $\varepsilon = 1$ if $h_g + h_d < H$, and $\varepsilon = 0$ if $h_g + h_d = H$.

We write equation (1) and equation (2) in its dimensionless form by scaling h_g, h_d and x by the aquifer height H, and we scale t by the characteristic time

$$T_c = \frac{H\phi}{\kappa\lambda_d\Delta\rho_{wd}g}. \tag{5}$$

The dimensionless equations are then given by

$$\frac{\partial\tilde{h}_g}{\partial\tilde{t}} + \frac{1}{(1-S_{wc}-S_{gr}\tilde{R})}\frac{\partial}{\partial\tilde{x}}\left[\delta(1-\tilde{f}_g)\tilde{h}_g(\sin\theta - \cos\theta\frac{\partial\tilde{h}_g}{\partial\tilde{x}} - \frac{\partial\tilde{h}_c}{\partial\tilde{x}}) + \tilde{f}_g\tilde{h}_d(\sin\theta + \cos\theta\frac{\partial\tilde{h}_d}{\partial\tilde{x}})\right] = -\tilde{D}, \tag{6}$$

$$\frac{\partial\tilde{h}_d}{\partial\tilde{t}} - \frac{\partial}{\partial\tilde{x}}\left[\delta\tilde{f}_d\tilde{h}_g(\sin\theta - \cos\theta\frac{\partial\tilde{h}_g}{\partial\tilde{x}} - \frac{\partial\tilde{h}_c}{\partial\tilde{x}}) + (1-\tilde{f}_d)\tilde{h}_d(\sin\theta + \cos\theta\frac{\partial\tilde{h}_d}{\partial\tilde{x}})\right] = \frac{\tilde{D}}{\chi_v}(1-S_{wc}-S_{gr}\tilde{R}), \tag{7}$$

where we have defined two additional dimensionless parameters

$$\delta = \frac{\lambda_g\Delta\rho_{gw}}{\lambda_d\Delta\rho_{wd}}, \quad \tilde{D} = \frac{q_d}{\kappa\lambda_d\Delta\rho_{wd}g}\varepsilon. \tag{8}$$

3. Model Application

We now use the model to investigate the interplay between residual trapping, solubility trapping, and capillary pinning in the context of large-scale carbon sequestration. *MacMinn & Juanes* (2013) [16] studied the effects of residual trapping and solubility trapping and demonstrated that the combination of the two mechanisms always traps the CO_2 much more effectively than either mechanism alone. Here, we study the impact of capillary pinning as an additional trapping mechanism by modeling the post-injection migration of a CO_2 current in the Paluxy Sandstone located in the East Text Basin. The aquifer and the CO_2/brine properties associated with the Paluxy Sandstone are presented in *Szulczewski et al.* (2012) [20] and summarized in Table 1 below. Specifically, we compare the lifetime of the spreading CO_2 current and its maximum migration distance with and without the influence of capillary pinning.

We assume that CO_2 is injected uniformly along a linear, 200 km array of wells, and we model the evolution of the planar cross-sectional profile of the resulting CO_2 current. The shape of the CO_2 current at the end of injection can be described by the analytical equation below [11,12,22],

$$\tilde{h}_g(\tilde{x}) = \frac{\sqrt{\frac{lM_{gw}}{H\tilde{x}}} - 1}{M_{gw} - 1}, \tag{9}$$

where $M_{gw} = \mu_w / \mu_g$ is the viscosity ratio between CO_2 and the ambient brine, l is the characteristic length scale of the injected CO_2. The product of l and H equals to the initial cross-sectional area of the CO_2 current. We use the solution to Equation 9 as the initial condition for our model.

Table 1. Model input parameters for the Paluxy Sandstone.

	Bo^{-1}	κ	ϕ	θ	S_{gr}	H	$\Delta\rho_{gw}$	$\Delta\rho_{wd}$	μ_g	μ_d	χ_v
Paluxy Sandstone	[-]	m^2	[-]	[°]	[-]	[m]	[kg/m^3]	[kg/m^3]	[mPa-s]	[mPa-s]	[-]
	1.89E-02	3E-13	0.20	1	0.3	15	400	6	0.06	0.8	0.05

Figure 1 shows the post-injection migration of 7.2 Mt of injected CO_2 in the Paluxy Sandstone. The CO_2 current is subject to residual trapping and solubility trapping here, but the effects of capillary pinning are not included. In this scenario, the CO_2 current reaches a maximum migration distance of 8.2 km at approximately 200,000 years, after which it starts to retreat due to continued dissolution. Figure 2 shows the post-injection migration of 7.2 Mt of CO_2 in the Paluxy Sandstone, under the same conditions as the simulation shown in Figure 1, except that capillary pinning is now included in the simulation. In this case, capillary pressure hysteresis pins an increasingly larger portion of the CO_2/brine interface as the CO_2 current migrates, until the entire current becomes pinned. Comparison with Figure 1 shows that the additional contribution of capillary pinning helps stop the migration of the CO_2 current much earlier (64,000 years), and at a shorter distance (5.9 km).

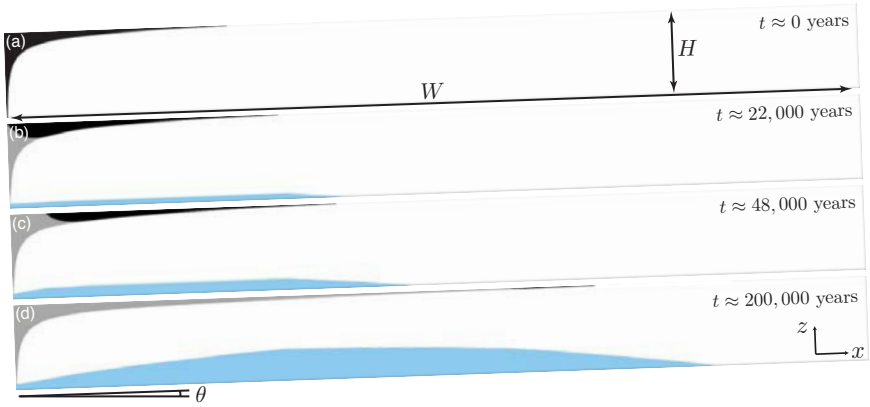

Fig. 1. Simulation of post-injection migration of 7.2 Mt tonnes of injected CO_2 in the Paluxy Sandstone, without including the effects capillary pinning. After injection stops, the buoyant CO_2 current (black) migrates up-dip, leaving behind a trail of residually trapped CO_2 blobs in its wake (grey). CO_2 is also dissolved into the ambient brine due to convective mixing, forming a dense mound of brine saturated with dissolved CO2 (blue). CO_2 and brine are assumed to be completely miscible here and capillarity is ignored. Note that the vertical scale of the aquifer is greatly exaggerated in the figure. The aspect ratio of the model domain is $W/H = 800$. The CO_2 current reaches its maximum migration distance after approximately 200,000 years (d), after which it starts to retreat due to continued dissolution.

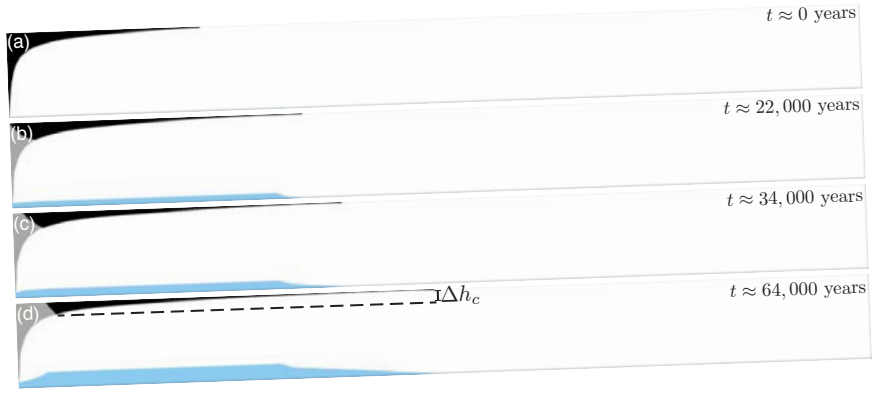

Fig. 2. Simulation of post-injection migration of 7.2 Mt tonnes of injected CO_2 in the Paluxy sandstone, including the effects of capillary pinning. Capillary pressure hysteresis pins an increasingly larger portion of the CO_2/brine interface as the CO_2 current migrates, until the entire current becomes pinned (d). Complete pinning of the CO_2/brine interface corresponds to a CO_2 current thickness of Δh_c, at which point the current lacks the necessary hydrostatic pressure to overcome capillary pressure hysteresis and stops spreading. Comparison with Figure 1 shows that the additional contribution of capillary pinning help stop the migration of the CO_2 current earlier (t ≈ 64,000 years), and at a shorter distance.

When the CO_2 current reaches its maximum migration distance, the previously mobile CO_2 is either residually trapped, dissolved into the ambient brine, or immobilized by capillary pinning. We investigate the varying contribution of each of the trapping mechanisms at the end of the mobile CO_2 current's lifetime, as a function of the amount of CO_2 injected (Figure 3). We find that the majority of the CO_2 is trapped by capillary pinning. However, capillary pinning does become less important as a larger amount of CO_2 is injected, whereas solubility trapping becomes more important. This can be attributed to the fact that convective dissolution occurs only at the CO_2-brine interface. A larger amount of injected CO_2 creates a longer CO_2-brine interface, which enhances solubility trapping.

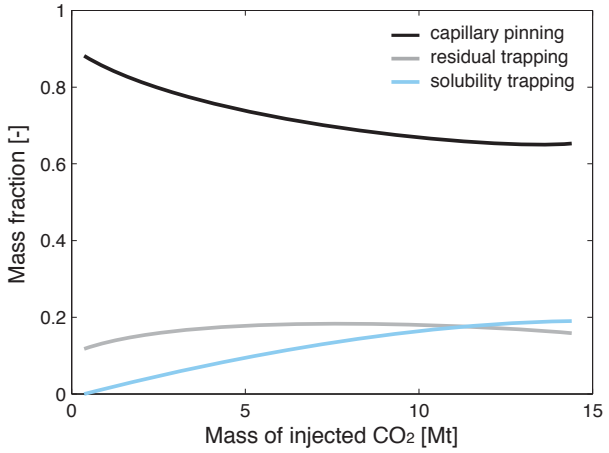

Fig. 3. Mass fraction of CO_2 immobilized by capillary pinning, residual trapping, and solubility trapping, as a function of the amount of CO_2 injected.

We have presented a model for the post-injection migration of CO_2 gravity currents in a confined, sloping aquifer, subject to residual trapping, solubility trapping, and capillary pinning. We have shown that residual trapping, solubility trapping, and capillary pinning complement each other to limit the maximum migration distance, as well as the duration of migration of a buoyant CO_2 current. The relative contribution of residual trapping, solubility trapping, and capillary pinning varies as a function of the total amount of CO_2 injected.

References

[1] Lackner, K. S. (2003), Climate change: a guide to CO_2 sequestration. Science, 300(5626):1677–1678.

[2] Schrag, D. P. (2007), Preparing to capture carbon. Science, 315(5813):812–813.

[3] Orr, F. M. (2004), Storage of carbon dioxide in geological formations. Journal of Petroleum Technology, (9):90–97.

[4] IPCC. Carbon Dioxide Capture and Storage (2005). Special Report prepared by Working Group III of the Intergovernmental Panel on Climate Change, Cambridge, UK.

[5] MacMinn, C. W. (2008), Analytical modeling of CO_2 migration in saline aquifers for geological CO_2 storage. Masters thesis, Massachusetts Institute of Technology.

[6] Orr, F. M. (2009), Onshore geologic storage of CO_2. Science, 325:1656–1658.

[7] Szulczewski, M. L., C. W. MacMinn, H. J. Herzog, and R. Juanes (2012). Lifetime of carbon capture and storage as a climate-change mitigation technology. Proc. Natl. Acad. Sci. , 109(14):5185–5189.

[8] Zhao B., C. W. MacMinn, M. L. Szulczewski, J. A. Neufeld, H. E. Huppert, and R. Juanes (2013), Interface pinning of immiscible gravity exchange flows in porous media, Phys. Rev. E, 87, 023015.

[9] Zhao B., C. W. MacMinn, H. E. Huppert, and R. Juanes (2014), Capillary pinning and blunting of immiscible gravity currents in porous media, Water Resour. Res., 2014WR015335.

[10] Hesse, M. A., F. M. Orr Jr., and H. A. Tchelepi (2008), Gravity currents with residual trapping, J. Fluid Mech., 611, 35–60.

[11] Juanes, R., C. W. MacMinn, and M. L. Szulczewski (2010), The footprint of the CO_2 plume during carbon dioxide storage in saline aquifers: Storage efficiency for capillary trapping at the basin scale, Transp. Porous Media, 82, 19–30.

[12] MacMinn, C. W., M. L. Szulczewski, and R. Juanes (2010), CO_2 migration in saline aquifers. Part 1: Capillary trapping under slope and groundwater flow, J. Fluid Mech., 662, 329–351.

[13] Gasda, S. E., J. M. Nordbotten, and M. A. Celia (2011), Vertically-averaged approaches for CO_2 migration with solubility trapping, Water Resour. Res., 47, W05528.

[14] MacMinn, C. W., M. L. Szulczewski, and R. Juanes (2011), CO_2 migration in saline aquifers. Part 2. Capillary and solubility trapping, J. Fluid Mech., 688, 321–351.

[15] MacMinn, C. W., J. A. Neufeld, M. A. Hesse, and H. E. Huppert (2012), Spreading and convective dissolution of carbon dioxide in vertically confined, horizontal aquifers, Water Resour. Res., 48, W11516.

[16] MacMinn, C. W., and R. Juanes (2013), Buoyant currents arrested by convective dissolution, Geophys. Res. Lett., 40, 2017–2022,

[17] Hidalgo, J.J., C. W. MacMinn, and R. Juanes (2013), Dynamics of convective dissolution from a migrating current of carbon dioxide, Adv. Water Resour., 62, 511–519.

[18] Hewitt D.R., J.A., Neufeld, J.R. Lister (2013), Convective shutdown in a porous medium at high Rayleigh number. J Fluid Mech., 719:551–86.

[19] Fu X., L. Cueto-Felgueroso, R. Juanes (2013), Pattern formation and coarsening dynamics in three-dimensional convective mixing in porous media. Philos. Trans. R. Soc. A., 371, 20120355

[20] Szulczewski M.L., M. A. Hesse, and R. Juanes (2013) Carbon dioxide dissolution in structural and stratigraphic traps. J Fluid Mech., 736: 287-315.

[21] Pau, G., J. B. Bell, K. Pruess, A. S. Almgren, M. J. Lijewski, and K. Zhang (2010), High- resolution simulation and characterization of density-driven flow in CO_2 storage in saline aquifers. Adv. Water Resour., 33(4):443–455.

[22] Nordbotten, J. M., Celia, M. A., Bachu, S. (2005) Analytical solution for CO_2 plume evolution during injection. Transp. Porous Media., 58: 339–360.